

Optimal Power Flow for DC Networks with Robust Feasibility and Stability Guarantees

Jianzhe Liu, *Member, IEEE*, Bai Cui, *Member, IEEE*, Daniel K. Molzahn, *Member, IEEE*,
Chen Chen, *Member, IEEE*, and Xiaonan Lu, *Member, IEEE*

Abstract—With high penetrations of renewable generation and variable loads, there is significant uncertainty associated with power flows in DC networks such that stability and constraint satisfaction are important concerns. Most existing DC network optimal power flow (DN-OPF) formulations assume exact knowledge about loading conditions and do not provide stability guarantees. In contrast, this paper studies a DN-OPF formulation which considers both stability and constraint satisfaction under uncertainty. The need to account for a range of uncertainty realizations in this paper’s robust optimization formulation results in a challenging semi-infinite program (SIP). The proposed solution algorithm reformulates this SIP into a computationally amenable problem whose solution provides a feasible operating point for the SIP. This algorithm constructs a convex stability set using sufficient conditions for the existence of a feasible and stable power flow solution. Solving an optimization problem based on this convex stability set provides generator set points which ensure that the DC network has a stable operating point for any considered uncertainty realization. This optimization problem takes a form similar to a deterministic DN-OPF problem and is therefore tractable. The proposed algorithm is demonstrated using various DC networks adapted from IEEE test cases.

I. INTRODUCTION

A DC network is a power system with electrical power flows in the form of direct current [1]. DC networks have found promising applications in low- and medium-voltage power systems with high penetrations of DC loads and generators, such as distribution systems, microgrids, shipboard electrical networks, data centers, etc. [2].

An operating point for a DC network satisfies the network’s power flow equations. System operators seek the optimal operating point which maximizes economic efficiency while satisfying various physical and operational constraints [2]. The optimal operating point can be found by solving an optimal power flow (OPF) problem [3]. For AC power systems, the OPF problem has recently been shown to be NP-hard [4]. Many research efforts have attempted to improve the tractability of AC-OPF problems using various approximations and relaxations of the power flow equations [5].

Recent research has studied OPF problems for DC networks (DN-OPF) [6]–[13]. Note that DN-OPF problems are very dif-

ferent from OPF problems for AC systems that use the linear “DC” power flow approximation to obtain linear programming formulations (often termed DC-OPF problems [14]). Rather, DN-OPF problems incorporate the nonlinear power flow equations associated with DC networks, resulting in non-convex optimization problems [11].

A variety of methods have been applied to solve DN-OPF problems. In [6], a genetic algorithm is applied to solve the OPF problem for a DC distribution system. In [7], linearization techniques are used to simplify the problem. Other methods [8]–[10] employ second-order cone programming and quadratic convex programming to relax a DN-OPF problem into a convex formulation. This existing work demonstrates the capability to effectively solve various DN-OPF problems.

Despite recent advances, existing work [7]–[10] has two major limitations. First, previous results primarily focus on deterministic DN-OPF problems where the loading conditions are assumed to be fixed and known *a priori*. Second, previous results do not consider the stability characteristics of DN-OPF solutions. Nevertheless, with high penetrations of intermittent generation and variable loads, uncertainty in the net loading conditions is a characteristic feature of DC networks [15]. Ensuring stability despite this uncertainty is a key concern for secure and reliable operation of DC networks [16], [17]. The lack of stability considerations when choosing an operating point may result in instability. Moreover, directly applying the OPF decisions computed using a specific scenario to an uncertain system can cause unpredictable deviations of the system operating point from the designated value [18], [19]. This may lead to violations of operational constraints and possibly cause voltage collapse [20], [21], where the power flow equations no longer admit a solution.

We propose a robust stability-constrained DN-OPF algorithm to address these limitations. We focus on a generic DC network with nonlinear constant power loads (CPLs) whose demands have interval uncertainties [2]. We seek to select the generators’ voltage set points in order to minimize operational costs while ensuring the existence of stable and secure operating points for all realizations of the uncertain loading conditions. In other words, solutions resulting from our algorithm guarantee: 1) robust stability (local exponential stability of the operating point) and 2) robust feasibility (existence of power flow solutions) and security (the satisfaction of all other operational constraints).

To provide robust stability and feasibility guarantees, we formulate a DN-OPF problem that incorporates uncertainty and stability conditions. Solving this problem is difficult. First,

J. Liu, B. Cui, and C. Chen are with the Energy Systems Division, Argonne National Laboratory, Lemont, IL 60439, USA. Emails: jianzhe.liu@anl.gov, bcui@anl.gov, and morningchen@anl.gov.

D. Molzahn is with the School of Electrical and Computer Engineering, Georgia Institute of Technology, Atlanta, GA 30332, and also with the Energy Systems Division, Argonne National Laboratory, Lemont, IL 60439, USA. Email: molzahn@gatech.edu.

X. Lu is with the College of Engineering, Temple University, Philadelphia, PA 19122. Email: xiaonan.lu@temple.edu.

existing stability conditions for DC networks are developed to study given operating points [22]; hence, ensuring stability when operating points are decision variables is challenging. Additionally, to ensure robustness, the power flow equation along with the stability condition need to jointly hold for all uncertainty realizations. This results in a semi-infinite programming (SIP) problem [23] that is generally computationally intractable [24]. There exist methods, like the minimax robust optimization approach [25] and scenario methods [24], to solve a convex SIP problem by transforming it into a more tractable problem. Nevertheless, existing approaches either cannot guarantee the existence of a solution to the original problem or are computationally expensive [26].

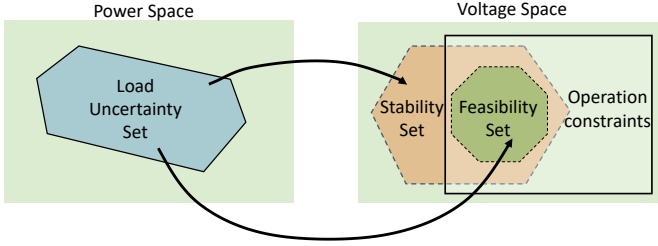


Fig. 1. Illustration of the proposed work.

The proposed algorithm converts the SIP problem into a tractable formulation that resembles a well-studied DN-OPF problem. Fig. 1 illustrates the key idea of the proposed work. The main technical tasks are summarized as:

- (1) For a given polytopically constrained uncertainty set for the loads, we first derive a polytopic stability set in the voltage space such that any operating point therein is guaranteed to be stable.
- (2) We study the solvability of the DC network power flow equations to certify the unique existence of an operating point in a feasibility set, for a given load profile. This feasibility set depends on generator voltage set points and the loads.
- (3) By solving a tractable problem reminiscent of a DN-OPF problem, we compute generator voltage set points which ensure that the feasibility sets associated with all uncertainty realizations in the given load uncertainty set are contained within the intersection of the stability set and an operational constraint set. This guarantees robustly stable and robustly feasible operation.

Using existing stability analysis results [22], we first certify whether a given polytope in the voltage space is a stability set using a linear matrix inequality (LMI) feasibility test. With an initial polytope set, we can find an optimal scaling of its size to determine the largest stability set with respect to the initial set. The scaling can be efficiently found by solving a generalized eigenvalue problem [27]. We then employ AC power flow feasibility results [28] to derive a condition which ensures that the DC network power flow equation always has a solution lying in a polytope whose center and radius depend on the generators' voltage set points. Lastly, we formulate a DN-OPF problem to optimally design the voltage set points so that the operating points for all uncertainty realizations are always

within the intersection of the stability set and operational constraint set. The problem is tractable and resembles ordinary DN-OPF problems studied in the literature [8]. We prove that any solution of this tractable problem is a feasible point of the original intractable SIP problem. Therefore, the solution guarantees robust feasibility and stability. To the best of our knowledge, this work is among the first to solve an OPF problem with robust stability and feasibility guarantees which does not rely on simplifying assumptions such as special load models [18] or power flow solution existence [19].

The rest of the paper is organized as follows: Section II first introduces notation and the steady-state and dynamic models of a DC network and then formulates the problem considered in this paper. Section III discusses the development of the proposed algorithm. Section IV demonstrates the efficacy of the proposed work using case study simulations. Section V concludes the paper and discusses future research directions.

II. SYSTEM MODELING AND PROBLEM STATEMENT

A. Notation

In this paper, we use $\mathbf{1}$ and $\mathbf{0}$ to represent vectors of all 1's and 0's of appropriate sizes, and use I to represent the identity matrix of appropriate size. Recall that a square matrix A is Hurwitz if all real parts of its eigenvalues are negative. In addition, we use $A_{j,k}$ to denote the element on the j -th row and k -th column. For a vector v , let v_k represent its k -th element. Let operator $\text{diag}\{v\}$ yield a diagonal matrix with the vector's components being the diagonal entries. For a real square matrix A , A^{-1} denote its inverse and $A \succ 0$ means it is symmetric positive definite.

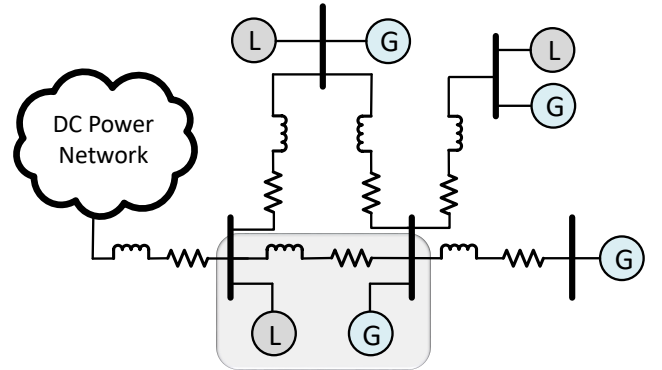


Fig. 2. Example DC power network.

B. DC Power Systems

In this paper, we focus on a DC network with n_s generators, n_ℓ loads, and n_t power lines. The total number of these components is $n = n_s + n_t + n_\ell$. Let the index sets of generators, loads, and power lines be \mathcal{N}_s , \mathcal{N}_ℓ , and \mathcal{E}_t , respectively. Fig. 2 shows an example DC network consisting of lumped π -equivalent models [29] where generators and loads are interconnected via equivalent RLC circuits [1].

1) *Load and Generator Models*: Fig. 3 shows a zoomed-in image of one part of the circuit. Suppose the circuit has the k -th generator, p -th power line, and j -th load. Let $i_{to}(t)$ and $i_{td}(t)$ represent the current flowing into and out of the circuit.

Loads are modeled as constant power loads (CPLs) that are connected in parallel with a lumped shunt resistor by Norton's Theorem. It is well known that a CPL is a nonlinear load and its negative impedance effect is a major source of instability in a DC network [30], [31]. It is modeled as a nonlinear current sink with current injection equal to the power demand divided by terminal voltage. For the j -th load, let p_{lj} represent its power output, and let v_{lj} represent the terminal voltage. At the nominal condition, $p_{lj} = p_{lj}^*$, where p_{lj}^* is a given constant. Each p_{lj} can be considered as a perturbation to p_{lj}^* that is unknown and bounded within a given uncertainty interval $[p_{lj}, \bar{p}_{lj}]$ where $\bar{p}_{lj} \geq p_{lj}$. The uncertainty interval may stem from probabilistic measures of demand fluctuations or from the physical capacity constraints of loads. Let \mathcal{P}_ℓ be the polytopic uncertainty set for all load, that is, $\mathcal{P}_\ell = \{p_\ell : p_{lk} \in [p_{lk}, \bar{p}_{lk}], k \in \mathcal{N}_\ell\}$. Let R_{lj} and C_{lj} represent the load resistance and capacitance, respectively.

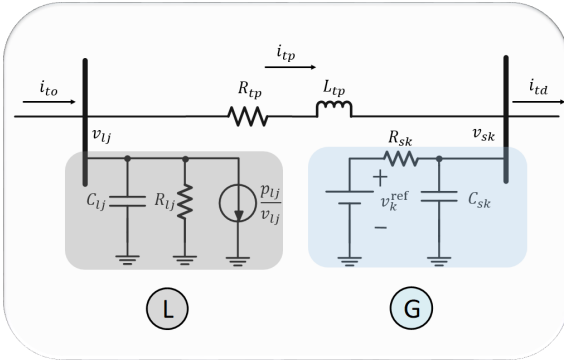


Fig. 3. Zoomed-in image of the dynamic circuit.

Remark 1. Generators are modeled as voltage sources [29] that are in series with equivalent resistors by Thévenin's Theorem. We assume that proper low-level controllers [2] have been employed to regulate the terminal voltage of a generator to track a reference set point. Consequently, the generator can automatically vary power outputs to respond to changing loading conditions. The generator internal dynamics, including those from low-level controllers and electromechanical transients, are not considered in this paper, and we mainly focus on the network dynamics contributed by electromagnetic transients in the stability analysis. Nevertheless, the main results of the paper can be extended to include various generator dynamics as well. For the k -th source, let v_k^{ref} be the controllable voltage set point, v_{sk} be the external generator voltage, and R_{sk} , C_{sk} represent the source resistance and capacitance, respectively. We impose operational constraints on v_k^{ref} such that vector v^{ref} which includes all voltage set points needs to lie in a given convex constraint set \mathcal{V}^{ref} .

The main results of this paper can be extended to DC networks with other generator and load models. For example,

constant-current and constant-impedance loads are linear and can be easily incorporated in the model. Additionally, for generators with V-I droop control [2], the voltage set point can be considered as the droop reference and the droop gains can be modeled as virtual impedances that are included in the RLC circuits.

2) *Dynamic Network Model*: Sources and loads are connected to DC buses. The buses form a connected graph where a bus is a node and an edge is a π -equivalent power line. For the p -th power line, let $i_{tp}(t)$ be the current flow and let R_{tp} and L_{tp} represent line resistance and inductance. In this paper, the dynamics of the system are mainly associated with the RLC circuit that connects all the components [1]. Note that some dynamic controllers have recently been developed for DC networks [2]. Our results can be easily extended to cover the additional dynamics introduced by these controllers.

We exemplify the modeling approach using the circuit shown in Fig. 3. The state variables of the example circuit are the voltages of the capacitors and the currents through the inductors, namely, $v_{sk}(t)$, $v_{lj}(t)$, and $i_{tp}(t)$. The design variable is the output voltage of the source, v_k^{ref} . The dynamics of the circuit are represented by the following model using Kirchhoff's current and voltage laws,

$$\dot{i}_{tp}(t) = \frac{1}{L_{tp}} (v_{sk}(t) - R_{tp}i_{tp}(t) - v_{lj}(t)), \quad (1a)$$

$$\dot{v}_{sk}(t) = \frac{1}{C_{sk}} \left(\frac{v_k^{\text{ref}} - v_{sk}(t)}{R_{sk}} + i_{to}(t) - i_{tk}(t) \right), \quad (1b)$$

$$\dot{v}_{lj}(t) = \frac{1}{C_{lj}} \left(-\frac{v_{lj}(t)}{R_{lj}} - i_{td}(t) + i_{tk}(t) - \frac{p_{lj}}{v_{lj}(t)} \right). \quad (1c)$$

The first two equations in (1) characterize the behavior of the power line and the source. They are linear in the state variables and the design variable. However, the last equation is nonlinear due to the term, $p_{lk}/v_{lk}(t)$. Recall that $i_{to}(t)$ and $i_{td}(t)$ represent aggregate line currents flowing to the load and from the source, respectively, and they have similar dynamics to those of $i_{tk}(t)$.

The modeling approach can be applied to the entire system. By dropping the subscripts indicating variable indices, $p_\ell, v_\ell, v_s, i_t, v^{\text{ref}}$ represent the vectors of load powers, load voltages, generator external voltages, power line currents, and controllable voltage set points, respectively. Let $x = [i_t^\top, v_s^\top, v_l^\top]^\top$ be the vector of state variables and $h(x, p_\ell) = [p_{\ell 1}/v_{\ell 1}, \dots, p_{\ell n_\ell}/v_{\ell n_\ell}]^\top$, where $(\cdot)^\top$ is the transpose.

With the above description and notation, the overall dynamics of the DC grid can be written as follows:

$$\dot{x}(t) = Ax(t) + Bv^{\text{ref}} + Ch(x(t), p_\ell), \quad p_\ell \in \mathcal{P}_\ell, \quad (2)$$

where the matrices $A \in \mathbb{R}^{n \times n}$, $B \in \mathbb{R}^{n \times n_s}$, and $C \in \mathbb{R}^{n \times n_\ell}$ are constant matrices that are determined by the network topology and RLC circuit parameters through similar methods to those in [22]. This is a well-accepted model for DC network stability studies that is applicable to a variety of DC power systems [2], [32], [33], for instance, DC transmission systems [32].

Let $x^e = [(i_t^e)^\top, (v_s^e)^\top, (v_\ell^e)^\top]^\top \in \mathbb{R}^n$ be an equilibrium of (2). For $v_{\ell j}^e \neq 0, \forall j \in \mathcal{N}_\ell$, system (2) can be linearized around x^e as

$$\dot{x}(t) = J(v_\ell^e, p_\ell)x(t), \quad (3)$$

where it can be easily verified that the corresponding Jacobian matrix $J(v_\ell^e, p_\ell)$ is a function of p_ℓ and v_ℓ^e . In other words, the stability of an equilibrium only depends on the CPL power and steady-state CPL voltage. Specifically, the Jacobian matrix contains terms in the form of $p_{\ell j}/(v_{\ell j}^e)^2$.

We know from [34, Sect. 4.3] that the equilibrium is asymptotically stable if there exists a matrix $P = P^\top \succ 0$ that satisfies the following condition:

$$PJ(v_\ell^e, p_\ell) + J(v_\ell^e, p_\ell)^\top P \prec 0. \quad (4)$$

If p_ℓ and v_ℓ^e are given, this condition is a linear matrix inequality (LMI) constraint. However, in our problem, p_ℓ is uncertain, v_ℓ^e is unknown, and the coupling between p_ℓ , v_ℓ^e , and P is non-polynomial.

3) *Power Flow Model*: The power flow model describes the steady-state behavior at an operating point of a DC network. The power flow model is obtained by setting the left-hand side of (2) to $\mathbf{0}$ and rearranging terms as

$$p_\ell = \text{diag}\{v_\ell^e\} (Y_{\ell\ell}v_\ell^e + Y_{\ell s}v^{\text{ref}}), \quad (5)$$

where the terms in parentheses represent current injections. The connectivity between CPL-source and CPL-CPL are described by two admittance matrices $Y_{\ell s} \in \mathbb{R}^{n_\ell \times n_s}$ and $Y_{\ell\ell} \in \mathbb{R}^{n_\ell \times n_\ell}$ [17], which are submatrices of the system admittance matrix Y . Equation (5) is quadratic in state variables v_ℓ^e and bilinear in design variables v^{ref} and state variables v_ℓ^e .

C. Problem Statement

Recall that the Jacobian $J(v_\ell^e, p_\ell)$ depends on system operating points and uncertain loading conditions. From power flow equation (5), an operating point depends on the generators' voltage set points. Therefore, a poorly designed v^{ref} may 1) render the stability of system (2) at risk, and 2) make (5) admit no solution.

The goal of this work is to choose the value of v^{ref} which results in the minimum operating cost at the nominal condition while guaranteeing that the system is robustly feasible and stable. We make the terms *robustly feasible* and *robustly stable* precise in Definition 1 below:

Definition 1. Given generator voltage set point v^{ref} , system (2) is said to be *robustly feasible* if, for every $p_\ell \in \mathcal{P}_\ell$, it admits an equilibrium x^e which satisfies all operational constraints. The system is said to be *robustly stable* if, for every $p_\ell \in \mathcal{P}_\ell$, there exists a corresponding v_ℓ^e such that the Jacobian $J(v_\ell^e, p_\ell)$ is Hurwitz.

Desirable operating points for power systems are usually computed by solving optimal power flow (OPF) problems [3]. Recently, OPF problems for DC networks (DN-OPF) have been studied as well [7]–[10]. The formulation of existing DN-OPF problems can be summarized as follows,

$$\text{DN-OPF}^*: \quad \min_{v^{\text{ref}}} f(v^{\text{ref}}, v_\ell^{e*}), \text{ subj. to} \quad (6a)$$

$$(5), \quad p_\ell = p_\ell^*, \quad (6b)$$

$$v_\ell^e \in \mathcal{V}_\ell^e, \quad v^{\text{ref}} \in \mathcal{V}^{\text{ref}}, \quad (6c)$$

where $p^* \in \mathbb{R}^{n_\ell}$ and $v_\ell^{e*} \in \mathbb{R}^{n_\ell}$ are the CPL power profile and voltage at the nominal condition, $f: \mathbb{R}^{n_s} \times \mathbb{R}^{n_\ell} \rightarrow \mathbb{R}$ is usually a convex cost function representing the operating cost (e.g., power loss or generation cost), and $\mathcal{V}_\ell^e \subset \mathbb{R}^{n_\ell}$ is the convex operational constraint set of v_ℓ^e representing system operational requirements such as bounds on load voltages.¹

When the cost function is a quadratic function of the decision variables, problem (6) is a quadratically constrained quadratic program. Recently, effective methods have been developed to solve this problem [7]–[10] using approximation and convex relaxation techniques. However, problem (6) only considers a fixed loading condition and does not explicitly consider system stability. If the actual load is different from the nominal load, the system's operating point may be unexpected and possibly even unstable.

To address these limitations, we focus on the following problem with explicit constraints guaranteeing robust feasibility and robust stability:

$$\text{R. DN-OPF SIP:} \quad \min_{v^{\text{ref}}, P \succ 0} f(v^{\text{ref}}, v_\ell^{e*}), \text{ subj. to} \quad (7a)$$

$$(4), (5), (6c), \quad \forall p_\ell \in \mathcal{P}_\ell. \quad (7b)$$

Compared to problem (6), we add constraint (4) which is sufficient to provide stability guarantees. We also require all of the constraints to hold for any $p_\ell \in \mathcal{P}_\ell$ in order to ensure robust feasibility and robust stability in the presence of uncertainty. Existing methods for (6) cannot be directly applied to (7).

Problem (7) is intractable in general due to the infinite number of constraints on the decision variables used to ensure robust feasibility and stability. This makes (7) a semi-infinite programming (SIP) problem [25]. Finding a tractable reformulation for the SIP problem (7) is challenging due to non-convexity of the stability condition (4) and the power flow equations (5).

III. TRACTABLE DN-OPF WITH ROBUST FEASIBILITY AND STABILITY GUARANTEES

This section presents our algorithm for transforming the computationally forbidding problem (7) into a tractable formulation. As illustrated in Fig. 1, the algorithm involves three major steps: First, we formulate a computationally efficient optimization problem to find a set of v_ℓ^e that satisfies (4) for all $p_\ell \in \mathcal{P}_\ell$. Second, we develop a sufficient condition to show the existence of v_ℓ^e in a set depending on the voltage set points v^{ref} . Third, we develop a DN-OPF problem whose solution v^{ref} steers v_ℓ^e into a desired set.

¹We limit our presentation to only consider the state constraints related to the load voltages, which are directly relevant to the system stability, in order to simplify the paper's discussion. Other state variables are linear functions of the load voltages and the voltage set points of the generators. The proposed algorithm can be easily extended to incorporate constraints on these variables.

A. Robust Stability Set

To compute a set of v_ℓ^e that can satisfy (4), it suffices to find a convex inner approximation of the feasibility region of (4). For every $j \in \mathcal{N}_\ell$, let $\bar{v}_{\ell j}^e$ and $\underline{v}_{\ell j}^e$ be the upper and lower bounds of $v_{\ell j}^e$. In this paper, we assume that $\underline{v}_{\ell j}^e > 0$ to allow only positive steady-state voltages [35]. Let $\mathcal{V}_\ell^s = \{v_\ell^e : \underline{v}_{\ell j}^e \leq v_{\ell j}^e \leq \bar{v}_{\ell j}^e, \forall j \in \mathcal{N}_\ell\}$ be a polytope of interest.

Definition 2. A set $\mathcal{V}_\ell^s \subseteq \mathbb{R}^{n_\ell}$ is called a *robust stability set* if there exists a positive definite matrix P that makes (4) satisfied for all $p_\ell \in \mathcal{P}_\ell$ and $v_\ell^e \in \mathcal{V}_\ell^s$.

We seek a common Lyapunov function $Q = x^\top P x$ which certifies that the Jacobian matrix, $J(v_\ell^e, p_\ell)$, is Hurwitz for any $p_\ell \in \mathcal{P}_\ell$ and $v_\ell^e \in \mathcal{V}_\ell^s$. We first transform the non-polynomial constraints (4) into bilinear matrix inequalities (BMIs). Then, we show that the infinite BMIs can be further reduced to a finite number of linear matrix inequalities (LMIs). Finally, we formulate a generalized eigenvalue problem (GEVP) [36] to compute a convex robust stability set.

1) *BMI*: For notational brevity, define $\delta_j \triangleq p_{\ell j}/(v_{\ell j}^e)^2$ for $j \in \mathcal{N}_\ell$ and let $\delta \in \mathbb{R}^{n_\ell}$ be the corresponding vector. Let δ_j be bounded by box constraints with upper and lower bounds defined by $\bar{\delta}_j = \bar{p}_{\ell j}/(\underline{v}_{\ell j}^e)^2$ and $\underline{\delta}_j = \underline{p}_{\ell j}/(\bar{v}_{\ell j}^e)^2$, respectively. Hence, δ is contained in a polytopic set defined by $\Delta = \{\delta : \underline{\delta}_j \leq \delta_j \leq \bar{\delta}_j\}$. Let δ_k^v be the vertices of the set Δ for $k \in \mathcal{M}^v \triangleq \{1, \dots, 2^{n_\ell}\}$.

Thus, the Jacobian matrix of (2) can be equivalently transformed into a function of δ , denoted by $J(\delta)$. It can be easily checked that $J(\delta) = A + D \text{diag}\{\delta\}$, where D is an $n \times n_\ell$ matrix with $D_{kk} = 1/C_{\ell k}$ for $n_t + n_s \leq k \leq n$, and all the other elements are zero [22].

Since the Jacobian $J(\delta)$ is affine in δ , the stability condition (4) is implied by the following conditions, which are BMIs in P and δ :

$$PJ(\delta) + J(\delta)^\top P \prec 0, \quad \forall \delta \in \Delta. \quad (8)$$

2) *Infinite BMIs to Finite LMIs*: Since Δ is a polytope, the feasibility of BMIs (8) can be implied by the feasibility of the following finitely many constraints:

$$PJ(\delta_k^v) + J(\delta_k^v)^\top P \prec 0, \quad P = P^\top \succ 0, \quad k \in \mathcal{M}^v. \quad (9)$$

Since each δ_k^v is a constant vector, (9) is a convex LMI feasibility testing problem [27].

3) *Computational Complexity and Conservativeness*: The number of constraints in the LMI feasibility test (9) is exponential in the dimension of the uncertainty. Fortunately, there exist methods to reduce the number of constraints. For example, only one LMI needs to be checked to ensure the feasibility of (9). Let $\lambda > 0$, $\hat{A} = A + D \text{diag}\{(\bar{\delta} + \underline{\delta})/2\}$, and let $\delta^{\max} = (\bar{\delta} - \underline{\delta})/2$. In addition, let $\hat{C} = [0, \text{diag}\{\delta^{\max}\}]$ and $\hat{B} = [0; I]$. The feasibility of the following single LMI is a sufficient condition for the feasibility of (9) [37]:

$$\begin{bmatrix} P\hat{A} + \hat{A}^\top P + \lambda \hat{C}^\top \hat{C} & P\hat{B} \\ \hat{B}^\top P & -\lambda I \end{bmatrix} \prec 0, \quad P \succ 0, \quad \lambda > 0. \quad (10)$$

However, the improvement in computational tractability is accompanied by a rise in the conservativeness of the reformulated problem. One method to evaluate the conservativeness of

various conditions is to compare the volume of the largest sets that these conditions can certify as stability sets. Empirical studies show that the largest set that the single-LMI condition (10) can certify is only about 40% of the volume of the set obtained from the LMIs (9). Still, there exist methods to reduce the number of LMIs to be polynomially dependent on the dimension of the uncertainty [22], [26]. Numerical tests show that the resulting conditions can certify a set with a volume above 90% to that obtained from (9). These conditions thus have promising applicability for practical usage. Nevertheless, the transformation of LMIs (9) is out of scope for this paper. For the sake of brevity, we use (9) to present the numerical results in Section IV.

4) *Largest Robust Stability Set*: To determine the robust stability set, we simply need to find a choice for Δ that satisfies (8). Once Δ is determined, \mathcal{V}_ℓ^e can be conveniently derived based on the coupling between δ and v_ℓ^e .

An appropriate choice for Δ can be found by scaling an initial guess. The optimal scaling factor can be found by employing generalized eigenvalue problem (GEVP) techniques. Let the initial guess be $\Delta^0 = \{\delta : -\delta_j^0 \leq \delta_j \leq \delta_j^0\}$ where $\delta_j^0 > 0$.² Let $\alpha > 0$ be a scaling factor. We next find the largest α that makes (9) feasible.

Recall that $J(\delta) = A + D \text{diag}\{\delta\}$. The largest α can be found by solving the following GEVP problem:

$$\begin{aligned} \text{GEVP:} \quad & \min_{P \succ 0, \beta > 0} \beta, \quad \text{subj. to} \\ & G_k + \beta (PA + A^\top P) \prec 0, \quad k \in \mathcal{M}^v, \\ & PA + A^\top P \prec 0, \end{aligned} \quad (11)$$

where $G_k = P(D \text{diag}\{\delta_k^{v0}\}) + (D \text{diag}\{\delta_k^{v0}\})^\top P$, δ_k^{v0} is a vertex of Δ^0 , and $\beta = 1/\alpha$. Problem (11) is a quasi-convex problem that can be efficiently solved [27]. Additionally, for a given Δ^0 , (11) only requires knowledge of the system matrix A , which is based on the network topology and electrical parameters that are usually fixed. Hence, (11) can be solved once (off-line) prior to solving multiple DN-OPF problems with different loading conditions. A proper initial guess can also be determined before solving the DN-OPF problem. One applicable choice is letting $\delta_j^0 = \bar{p}_{\ell j}$. In many practical DC networks, the steady-state voltage levels of different buses are fairly close to each other [38]. The choice is effective when the voltage constraints are also fairly close to each other.

Based on the discussion above, the following condition characterizes the robust stability set:

Proposition 1. With given Δ^0 , if β is a solution of (11), \mathcal{V}_ℓ^s defined in the following expression is a robust stability set:

$$\mathcal{V}_\ell^s = \left\{ v_\ell^e : v_{\ell k}^e \geq \sqrt{\beta \cdot \bar{p}_{\ell j} / \delta_k^0} \right\}.$$

Note that the robust stability set only imposes a deterministic lower bound on each $v_{\ell k}^e$, meaning the feasibility region of (4) can be approximated by half planes. This observation is consistent with practical experience that higher voltage levels

²The choices for the upper and lower bounds on each δ_j do not need to be symmetric, in general. We choose symmetric bounds for the sake of simplicity.

are more preferable for maintaining stability, and thus provides implications for the design and operation of DC networks.

B. Feasibility Condition

Robust stability can only be guaranteed when there exists a power flow solution v_ℓ^e in $\mathcal{V}_\ell^s \cap \mathcal{V}_\ell^e$. We derive a condition to ensure such existence for any $p_\ell \in \mathcal{P}_\ell$ by leveraging a recent result on AC power flow solvability [28]: with fixed generator voltage set points v^{ref} , we characterize a compact set in \mathbb{R}^{n_ℓ} inside which a unique power flow solution v_ℓ^{e*} is guaranteed to exist for every $p_\ell \in \mathcal{P}_\ell$.

Given load power p_ℓ^* and a generator voltage set point v^{ref} , the nominal load voltage v_ℓ^{e*} is the solution of the following nominal power flow equation:

$$p_\ell^* = \text{diag}\{v_\ell^{e*}\} (Y_{\ell\ell} v_\ell^{e*} + Y_{\ell s} v^{\text{ref}}). \quad (12)$$

Furthermore, we define the open-circuit voltage vector $w \in \mathbb{R}^{n_\ell}$ and a dimensionless matrix $\tilde{Z}_{\ell\ell}$ as follows:

$$w \triangleq -Y_{\ell\ell} Y_{\ell s} v^{\text{ref}}, \quad \tilde{Z}_{\ell\ell} \triangleq \text{diag}\{w\}^{-1} Y_{\ell\ell}^{-1} \text{diag}\{w\}^{-1}. \quad (13)$$

The vector w can be viewed as the equivalent generator voltage seen by each load bus and $\tilde{Z}_{\ell\ell}$ is the impedance matrix normalized by the open-circuit voltages. Finally, denote the minimum normalized load voltage u^{\min} as $u^{\min} \triangleq \min_{j \in \mathcal{N}_\ell} \frac{v_{\ell j}^{e*}}{w_j}$.

Using the setup above, we restate the AC power flow solvability result from [28]:

Proposition 2 ([28, Thm. 1]). *Given load power p_ℓ^* , generator set point v^{ref} , and the corresponding power flow solution v_ℓ^{e*} satisfying $\|\tilde{Z}_{\ell\ell} p_\ell^*\|_\infty < (u^{\min})^2$, if the following inequality holds,*

$$\Gamma_s \triangleq \left(u^{\min} - \frac{\|\tilde{Z}_{\ell\ell} p_\ell^*\|_\infty}{u^{\min}} \right)^2 - 4 \|\tilde{Z}_{\ell\ell} (p_\ell^* - p_\ell)\|_\infty > 0, \quad (14)$$

the power flow equation (5) with load power p_ℓ admits a unique solution in

$$\mathcal{D}(p_\ell) = \left\{ v_\ell^e \in \mathbb{R}^{n_\ell} : |v_{\ell j}^e - v_{\ell j}^{e*}| \leq r w_j, j \in \mathcal{N}_\ell \right\}, \quad (15)$$

where

$$r \triangleq \frac{\left(u^{\min} - \frac{\|\tilde{Z}_{\ell\ell} p_\ell^*\|_\infty}{u^{\min}} \right) - \sqrt{\Gamma_s}}{2}. \quad (16)$$

Proposition 2 provides a sufficient condition which ensures the unique existence of a power flow solution in a polytope. When generator set points v^{ref} , the nominal load p_ℓ^* , and the power flow solution v_ℓ^{e*} are all given, the polytope will always be centered at v_ℓ^{e*} with a radius that is dependent only on p_ℓ .

C. Tractable Robust DN-OPF Formulation

With the robust stability set derived in Sections III-A and the feasibility condition derived in Section III-B, our objective now is to drive all $\mathcal{D}(p_\ell)$ into $\mathcal{V}_\ell^s \cap \mathcal{V}_\ell^e$.

With given p_ℓ^* and fixed v^{ref} , all sets $\mathcal{D}(p_\ell)$ are centered at the same v_ℓ^{e*} . The radius, on the other hand, is different. Intuitively, we can find the largest radius among these sets, and

correspondingly define a new set in the form of (15). Every $\mathcal{D}(p_\ell)$ must lie inside of this set.

It is easy to see from (14) and (16) that the quantities w , $\tilde{Z}_{\ell\ell}$, and u^{\min} only depend on v^{ref} and p_ℓ^* . For the radius, $r w_j$, r is dependent on p_ℓ such that it increases as $\|p_\ell^* - p_\ell\|_1$ increases. Therefore, to ensure robust feasibility, i.e., to ensure that for every $p_\ell \in \mathcal{P}_\ell$ there exists a power flow solution lying in $\mathcal{V}_\ell^s \cap \mathcal{V}_\ell^e$, we only need to ensure that $\mathcal{D}(p_\ell) \subseteq \mathcal{V}_\ell^s \cap \mathcal{V}_\ell^e$ for the value of p_ℓ that maximizes $\|p_\ell^* - p_\ell\|_1$. We denote such p_ℓ as p_ℓ^m , that is, $p_\ell^m = \arg \max_{p_\ell \in \mathcal{P}_\ell} \|p_\ell^* - p_\ell\|_1$. For a given \mathcal{P}_ℓ and p_ℓ^* , p_ℓ^m is a scalar constant that can be easily obtained by summing the largest element-wise deviations of uncertainty to the nominal value. With a change of variable, each largest element-wise deviation can be found by solving

$$\min_{p_{\ell j} \in [\underline{p}_{\ell j}, \bar{p}_{\ell j}], \gamma \geq 0} \gamma, \quad \text{subj. to: } |p_{\ell j}^* - p_{\ell j}| \leq \gamma.$$

Using p_ℓ^m , we seek to bound the variation of v_ℓ^e . Define

$$\bar{r} \triangleq \frac{\left(u^{\min} - \frac{\|\tilde{Z}_{\ell\ell} p_\ell^*\|_\infty}{u^{\min}} \right) - \sqrt{\Gamma_s}}{2}, \quad (17a)$$

$$\bar{\Gamma}_s \triangleq \left(u^{\min} - \frac{\|\tilde{Z}_{\ell\ell} p_\ell^*\|_\infty}{u^{\min}} \right)^2 - 4 \|\tilde{Z}_{\ell\ell} (p_\ell^* - p_\ell^m)\|_\infty > 0. \quad (17b)$$

It suffices to enforce the following constraints to ensure the existence of v_ℓ^e in $\mathcal{V}_\ell^s \cap \mathcal{V}_\ell^e$ for all p_ℓ :

$$v_{\ell j}^{e*} - \bar{r} w_j \geq \underline{v}_j, \quad v_{\ell j}^{e*} + \bar{r} w_j \leq \bar{v}_j, \quad j \in \mathcal{N}_\ell, \quad (18)$$

where \underline{v}_j and \bar{v}_j are element-wise load voltage bounds from $\mathcal{V}_\ell^s \cap \mathcal{V}_\ell^e$ for all $j \in \mathcal{N}_\ell$.

Notice that $\bar{r} w_j$ represents the largest deviation of a $v_{\ell j}^e$ to $v_{\ell j}^{e*}$. If (18) holds, there must be a v_ℓ^e lying inside of the desired set $\mathcal{V}_\ell^s \cap \mathcal{V}_\ell^e$.

The left-hand sides of (18) are functions of the nominal load voltage and generator set points. The right-hand sides are known constants derived from $\mathcal{V}_\ell^s \cap \mathcal{V}_\ell^e$. We can thus ensure satisfaction of (18) by finding proper values for the nominal load voltage and generator set points. Such values for v_ℓ^{e*} and v^{ref} are determined by solving the following DN-OPF problem:

$$\mathbf{R. DN-OPF*}: \min_{v^{\text{ref}}, u^{\min}} f(v^{\text{ref}}, v_\ell^{e*}), \quad \text{subj. to} \quad (19a)$$

$$(12), (13), (17), (18), \quad v^{\text{ref}} \in \mathcal{V}^{\text{ref}}, \quad (19b)$$

$$u^{\min} w_j \leq v_{\ell j}^{e*}, \quad j \in \mathcal{N}_\ell. \quad (19c)$$

In problem (19), recall that (12) denotes the power flow equations at the nominal condition. Constraints (13), (17), (18), and (19c) ensure satisfaction of the feasibility condition.

Remark 2. Problem (19) can be transformed into a quadratically constrained quadratic program (if $f(v^{\text{ref}}, v_\ell^{e*})$ is a quadratic function) similar to (6) in order to exploit existing solution algorithms. We only need to show that (17) can be equivalently transformed into quadratic constraints. Let s_{1j} be the j -th element of the vector $\tilde{Z}_{\ell\ell} p_\ell^*$ and let s_{2j} be the j -th element of the vector $\tilde{Z}_{\ell\ell} (p_\ell^* - p_\ell^m)$. From (13), both s_{1j} and s_{2j} are quadratic functions in v^{ref} . Let $a = \|\tilde{Z}_{\ell\ell} p_\ell^*\|_\infty$, $b = \|\tilde{Z}_{\ell\ell} (p_\ell^* - p_\ell^m)\|_\infty$, $c = \sqrt{\Gamma_s}$, and $d = a/u^{\min}$. For (17),

we can apply the following transformation based on change of variables:

$$2\bar{r} = (u^{\min} - d) - c, \quad c^2 = (u^{\min} - d)^2 - 4b, \quad (20a)$$

$$(u^{\min} - d)^2 > 4b, \quad d \cdot u^{\min} = a, \quad (20b)$$

$$a > s_{1j}, a > -s_{1j}, b > s_{2j}, b > -s_{2j}, j \in \mathcal{N}^\ell. \quad (20c)$$

It is straightforward to check that (20) only contains linear and quadratic constraints in the new variables a, b, c, d , and decision variables v^{ref} and u^{\min} .

From the solution of (19), we can also find the value of each $\bar{r}w_j$. According to (18), this provides bounds for v_ℓ^e that are valid for any $p_\ell \in \mathcal{P}_\ell$.

With given values of p_ℓ^m and the robust stability set \mathcal{V}^s , we state the main result of the paper as follows:

Theorem 1. *Any solution v^{ref} of problem (19) is a feasible point of SIP (7).*

Proof. It suffices to show that for all $p_\ell \in \mathcal{P}_\ell$, stability constraint (4) is satisfied, power flow equation (5) is feasible, and (6c) holds true with the solution of (19), v^{ref} .

Regarding any $p_\ell \in \mathcal{P}_\ell$, since v^{ref} makes (12), (13), (17), and (19c) satisfied, Proposition 2 shows that power flow equation (5) must admit a unique solution in $\mathcal{D}(p_\ell)$.

From the satisfaction of constraint (18), $\mathcal{D}(p_\ell)$ lies in \mathcal{V}^s , which shows that the power flow solution exists in the robust stability set. From Proposition 1 and Definition 2, stability constraint (4) is always satisfied.

In addition, it is easy to check that (6c) holds as well. This completes the proof. \square

Theorem 1 certifies that the solution to a tractable optimization problem (19) provides generator set points which guarantee robust feasibility and stability.

To summarize the results discussed in Sections II, III-A, and III-B, the proposed robust DN-OPF algorithm can be described with the following algorithm:

Algorithm 1 Find a feasible point, v^{ref} , for SIP (7)

Input: System matrices A, B, C, D , nominal load p_ℓ^* , load set \mathcal{P}_ℓ , constraint sets \mathcal{V}_ℓ^e and \mathcal{V}^{ref} , and cost function $f(v^{\text{ref}}, v_\ell^{e*})$.

Output: A solution v^{ref} .

Step 1: Select a Δ_0 and solve GEVP (11) to find α .

Step 2: Use α, Δ_0 , and \mathcal{P}_ℓ to find robust stability set \mathcal{V}_ℓ^s .

Step 3: Find $p_\ell^m = \arg \max_{p_\ell \in \mathcal{P}_\ell} \|p_\ell^* - p_\ell\|_1$.

Step 4: Solve problem (19) to find v^{ref} .

Each step in Algorithm 1 is computationally tractable. Propositions 1 and 2 along with Theorem 1 certify that the output of the algorithm solves SIP problem (7).

IV. CASE STUDIES

This section uses simulation case studies to demonstrate the effectiveness of the proposed algorithm. The simulations are conducted on a desktop with Intel Core i7 and 32GB of RAM. The optimization problems are solved using IPOPT [39], and the simulations are performed in Matlab/Simulink. We first

TABLE I
PARAMETERS FOR THE 14-BUS DC NETWORK CASE STUDY

R_{sk}	0.05 Ω	R_{lj}	5 Ω	R_{tp}	0.05 Ω
L_{tp}	3mH	C_{sk}	0.75mF	C_{lj}	0.9mF

show the efficacy and the limited conservativeness of the proposed work with a 14-bus system. We then demonstrate the computational efficiency of the proposed work.

A. Illustrative Case Study of a 14-Bus System

We first focus on an example DC network whose topology and bus types are the same as the IEEE 14-bus system. The parameters of the DC network given in Table I are chosen according to existing DC network case studies [17], [40]. The generators, loads, and power lines all have uniform parameters. We model all the eleven loads as unknown CPLs that can arbitrarily vary within the range [0, 50 kW]. The nominal load for each is 25 kW. All the five generators are controlled as voltage sources. Our algorithm is used to compute the voltage set points for the generators.

For this case study, we impose bounds of [425 V, 575 V] on the generator and CPL voltages. The objective function minimizes the losses at the nominal operating point.

Considering only on the nominal condition (ignoring the range of possible uncertainty realizations), the solution to the DN-OPF problem (6) yields set points of the five generators as 455.6, 462.9, 454.9, 454.4, and 460.0 V. We apply these set points and consider a uniform increase in load demands of 2.5 kW every 2.5 seconds. As shown in Fig. 4, the system becomes unstable at approximately 35 seconds when the loads are around 40 kW each. This shows the need to consider stability, especially in systems with significant uncertainties.

In comparison, we formulate the optimization problem (19) using our algorithm. Applying the stability analysis approach developed in Section III-A shows that the system is always robustly stable if the steady-state CPL voltage is higher than 500 V. Problem (19) yields the following set points: 544.5, 553.4, 543.8, 543.2, 549.9 V. Using these set points results in stability for the entire range of load demands when loads increase at the same rate as the previous testing, as shown in Fig. 5. This shows the efficacy of Theorem 1.

Moreover, Fig. 5 also demonstrates the limited conservativeness of the proposed algorithm. As discussed in Section III-C, we can find the bounds on the variation range of the operating points. Using the optimization results, we can certify that the ratio of an operating point to the nominal operating point lies in the range, [0.978, 1.022]. As shown in Fig. 5, the certified region is a reasonably tight estimation of the variations of system operating points.

B. Summary of Other Case Studies

We also tested the proposed algorithm on DC networks with the same topologies and bus types as the IEEE 9-, 30-, 39-, 69-, and 118-bus systems to study computational tractability. To summarize the results, Table II compares the average CPU

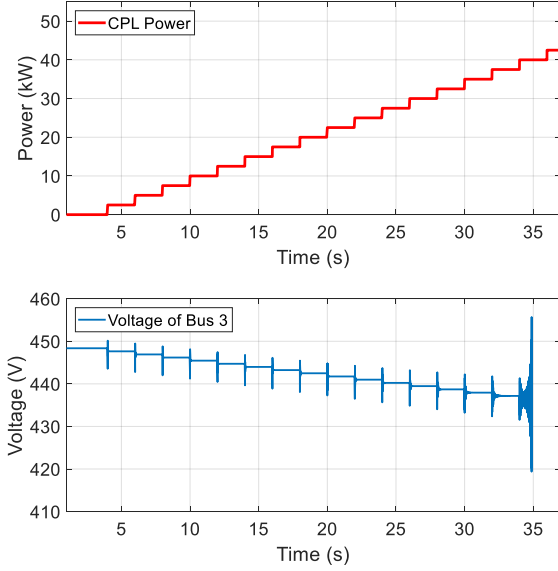


Fig. 4. DC network instability if only nominal DN-OPF is considered.

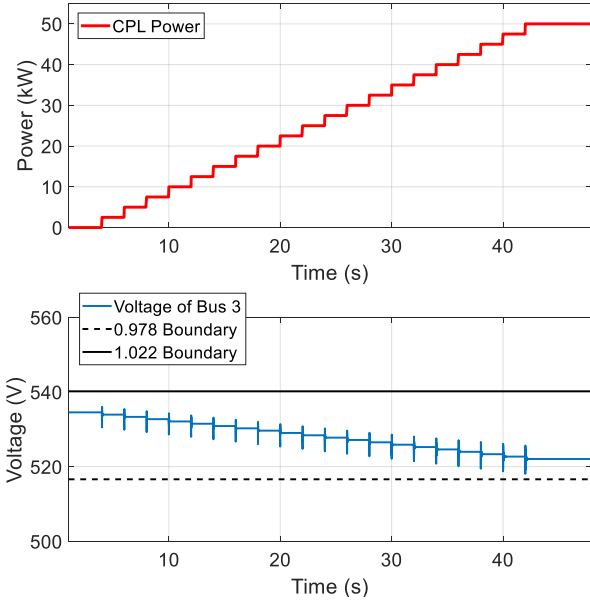


Fig. 5. DC network operation is stable for all conditions with the proposed algorithm.

time in IPOPT for solving problem (19) and the traditional DN-OPF problem (6), averaged over 10 tests for each system. Observe that the proposed optimization problem has a similar computational complexity as the traditional DN-OPF problem. This verifies the tractability of our algorithm.

V. CONCLUSION

This paper has developed a systematic algorithm to study stability-constrained OPF problems for DC networks under uncertainty. Such problems are usually intractable due to the involvement of infinitely many constraints. Our algorithm uses

TABLE II
COMPARISON OF COMPUTATION TIMES FOR SOLVING (6) AND (19)

	9-bus	30-bus	39-bus	69-bus	118-bus
DN-OPF (6)	0.10 s	0.11 s	0.31 s	0.91 s	1.40 s
Problem (19)	0.11 s	0.14 s	0.55 s	2.24 s	3.93 s

computationally efficient approaches to transform the problem into a tractable counterpart that resembles a traditional DN-OPF problem such that existing tools can be employed. We first derive a robust stability set within which any operating point is guaranteed to be robustly stable. We then use a sufficient condition which ensures the existence of feasible operating points in this set for all uncertainty realizations in the specified uncertainty set. The limited conservativeness and computational efficiency of the proposed algorithm is demonstrated using various test cases. In future research, we will investigate the application of the algorithm to DN-OPF problems with contingency constraints.

REFERENCES

- [1] F. Dörfler, J. W. Simpson-Porco, and F. Bullo, "Electrical networks and algebraic graph theory: Models, properties, and applications," *Proceedings of the IEEE*, vol. 106, no. 5, pp. 977–1005, 2018.
- [2] T. Dragičević, X. Lu, J. C. Vasquez, and J. M. Guerrero, "DC microgrids—Part I: A review of control strategies and stabilization techniques," *IEEE Transactions on Power Electronics*, vol. 31, no. 7, pp. 4876–4891, 2016.
- [3] M. B. Cain, R. P. O'Neill, and A. Castillo, "History of optimal power flow and formulations (OPF paper 1)," *US Federal Energy Regulatory Commission*, pp. 1–36, 2012.
- [4] K. Lehmann, A. Grastien, and P. Van Hentenryck, "AC-feasibility on tree networks is NP-hard," *IEEE Transactions on Power Systems*, vol. 31, no. 1, pp. 798–801, 2016.
- [5] D. K. Molzahn and I. A. Hiskens, "A Survey of Relaxations and Approximations of the Power Flow Equations," *Foundations and Trends in Electric Energy Systems*, vol. 4, no. 1-2, pp. 1–221, Feb. 2019.
- [6] M. Farasat *et al.*, "GA-based optimal power flow for microgrids with DC distribution network," in *IEEE Energy Conversion Congress and Exposition (ECCE)*, 2015, pp. 3372–3379.
- [7] O. D. Montoya, L. Grisales-Norena, D. González-Montoya, C. Ramos-Paja, and A. Garcés, "Linear power flow formulation for low-voltage DC power grids," *Electric Power Systems Research*, vol. 163, pp. 375–381, 2018.
- [8] L. Gan and S. H. Low, "Optimal power flow in direct current networks," *IEEE Transactions on Power Systems*, vol. 29, no. 6, pp. 2892–2904, 2014.
- [9] J. Li *et al.*, "Optimal power flow in stand-alone DC microgrids," *IEEE Transactions on Power Systems*, vol. 33, no. 5, pp. 5496–5506, 2018.
- [10] O. D. Montoya, W. Gil-González, and A. Garcés, "Optimal power flow on DC microgrids: A quadratic convex approximation," *IEEE Transactions on Circuits and Systems II: Express Briefs*, pp. 1–1, 2018.
- [11] A. Garcés, "On the convergence of Newton's method in power flow studies for DC microgrids," *IEEE Transactions on Power Systems*, vol. 33, no. 5, pp. 5770–5777, Sept. 2018.
- [12] W. Inam, J. A. Belk, K. Turitsyn, and D. J. Perreault, "Stability, control, and power flow in ad hoc DC microgrids," in *17th IEEE Workshop on Control and Modeling for Power Electronics (COMPEL)*, 2016, pp. 1–8.
- [13] J. Ma, L. Yuan, Z. Zhao, and F. He, "Transmission loss optimization-based optimal power flow strategy by hierarchical control for DC microgrids," *IEEE Transactions on Power Electronics*, vol. 32, no. 3, pp. 1952–1963, March 2017.
- [14] B. Stott, J. Jardim, and O. Alsac, "DC power flow revisited," *IEEE Transactions on Power Systems*, vol. 24, no. 3, pp. 1290–1300, 2009.
- [15] F. Cingoz, A. Elrayyah, and Y. Sozer, "Optimized settings of droop parameters using stochastic load modeling for effective DC microgrids operation," *IEEE Transactions on Industrial Applications*, vol. 53, no. 2, pp. 1358–1371, March 2017.

- [16] A. Riccobono and E. Santi, "Comprehensive review of stability criteria for DC power distribution systems," *IEEE Transactions on Industrial Applications*, vol. 50, no. 5, pp. 3525–3535, 2014.
- [17] Z. Liu, M. Su, Y. Sun, W. Yuan, H. Han, and J. Feng, "Existence and stability of equilibrium of DC microgrid with constant power loads," *IEEE Transactions on Power Systems*, vol. 33, no. 6, pp. 6999–7010, Nov. 2018.
- [18] R. Louca and E. Bitar, "Robust AC optimal power flow," *IEEE Transactions on Power Systems*, pp. 1–1, 2018.
- [19] D. K. Molzahn and L. A. Roald, "Towards an AC optimal power flow algorithm with robust feasibility guarantees," in *Power Systems Computation Conference (PSCC)*, 2018, pp. 1–7.
- [20] J. W. Simpson-Porco, F. Dörfler, and F. Bullo, "Voltage collapse in complex power grids," *Nature Communications*, vol. 7, p. 10790, 2016.
- [21] B. Cui and X. A. Sun, "A new voltage stability-constrained optimal power-flow model: Sufficient condition, SOCP representation, and relaxation," *IEEE Transactions on Power Systems*, vol. 33, no. 5, pp. 5092–5102, Sep. 2018.
- [22] J. Liu, W. Zhang, and G. Rizzoni, "Robust stability analysis of DC microgrids with constant power loads," *IEEE Transactions on Power Systems*, vol. 33, no. 1, pp. 851–860, Jan 2018.
- [23] R. Hettich and K. O. Kortanek, "Semi-infinite programming: Theory, methods, and applications," *SIAM Review*, vol. 35, no. 3, pp. 380–429, 1993.
- [24] J. M. Mulvey, R. J. Vanderbei, and S. A. Zenios, "Robust optimization of large-scale systems," *Operations research*, vol. 43, no. 2, pp. 264–281, 1995.
- [25] A. Ben-Tal and A. Nemirovski, "Robust optimization—Methodology and applications," *Mathematical Programming*, vol. 92, no. 3, pp. 453–480, 2002.
- [26] A. Ben-Tal, L. El Ghaoui, and A. Nemirovski, *Robust Optimization*. Princeton University Press, 2009, vol. 28.
- [27] S. Boyd and L. Vandenberghe, *Convex Optimization*. Cambridge University Press, 2004.
- [28] C. Wang, A. Bernstein, J.-Y. Le Boudec, and M. Paolone, "Explicit conditions on existence and uniqueness of load-flow solutions in distribution networks," *IEEE Transactions on Smart Grid*, vol. 9, no. 2, pp. 953–962, 2018.
- [29] J. A. Belk *et al.*, "Stability and control of ad hoc DC microgrids," in *IEEE 55th Annual Conference on Decision and Control (CDC)*, Dec. 2016, pp. 3271–3278.
- [30] L. Herrera, W. Zhang, and J. Wang, "Stability analysis and controller design of DC microgrids with constant power loads," *IEEE Transactions on Smart Grid*, vol. 8, no. 2, pp. 881–888, Mar. 2017.
- [31] N. Bottrell, M. Prodanovic, and T. C. Green, "Dynamic stability of a microgrid with an active load," *IEEE Transactions on Power Electronics*, vol. 28, no. 11, pp. 5107–5119, Nov. 2013.
- [32] G. O. Kalcon, G. P. Adam, O. Anaya-Lara, S. Lo, and K. Uhlen, "Small-signal stability analysis of multi-terminal VSC-based DC transmission systems," *IEEE Transactions on Power Systems*, vol. 27, no. 4, pp. 1818–1830, Nov. 2012.
- [33] A. Emadi *et al.*, "Constant power loads and negative impedance instability in automotive systems: Definition, modeling, stability, and control of power electronic converters and motor drives," *IEEE Transactions on Vehicular Technology*, vol. 55, no. 4, pp. 1112–1125, July 2006.
- [34] H. K. Khalil, *Nonlinear Systems*, 3rd ed. Upper Saddle River, NJ: Prentice Hall, 2002.
- [35] C. De Persis, E. R. A. Weitenberg, and F. Dörfler, "A power consensus algorithm for DC microgrids," *Automatica*, vol. 89, pp. 364–375, Mar. 2018.
- [36] S. Boyd, L. El Ghaoui, E. Feron, and V. Balakrishnan, *Linear Matrix Inequalities in System and Control Theory*. SIAM, 1994, vol. 15.
- [37] A. Ben-Tal and A. Nemirovski, *Lectures on Modern Convex Optimization: Analysis, Algorithms, and Engineering Applications*. SIAM, 2001, vol. 2.
- [38] J. W. Simpson-Porco, F. Dörfler, and F. Bullo, "On resistive networks of constant-power devices," *IEEE Transactions on Circuits and Systems II: Express Briefs*, vol. 62, no. 8, pp. 811–815, Aug 2015.
- [39] A. Wächter and L. T. Biegler, "On the implementation of an interior-point filter line-search algorithm for large-scale nonlinear programming," *Mathematical Programming*, vol. 106, no. 1, pp. 25–57, Mar. 2006.
- [40] D. Salomonsson and A. Sannino, "Low-voltage DC distribution system for commercial power systems with sensitive electronic loads," *IEEE Transactions on Power Delivery*, vol. 22, no. 3, pp. 1620–1627, July 2007.